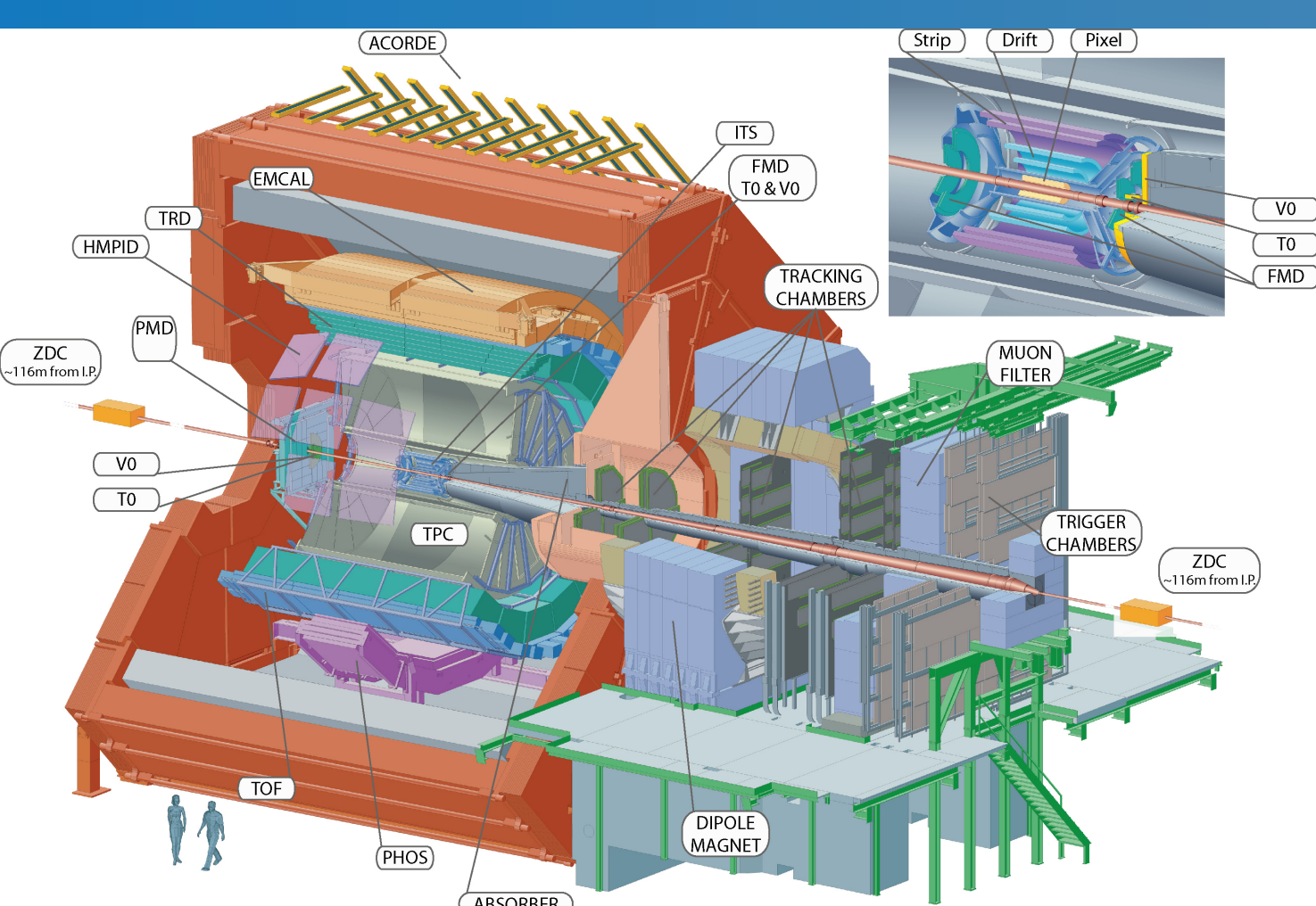


Physics motivation

- Charm quarks produced in hard scatterings at the initial stage of the collision → production cross section can be calculated within perturbative QCD, down to low transverse momentum.
- D-tagged jets → quark-jets enhanced sample;
 - measure jets from hard-scattering processes down to low transverse momentum.
- Pb-Pb collisions: provide new information about the heavy-quark energy loss mechanism, complementary to R_{AA} and v_2 studies.
- p-Pb and pp collisions: provide important reference for Pb-Pb measurements; test of theoretical models.

Tagging charm jets with D^{*+} mesons



p-Pb collisions at $\sqrt{s_{NN}} = 5.02$ TeV
98 M minimum-bias events

$D^{*\pm} \rightarrow D^0\pi^\pm$ (BR = $67.7 \pm 0.5\%$)
 $\rightarrow K^\pm\pi^-\pi^\pm$ (BR = $3.88 \pm 0.05\%$)
 $c\tau_{D^0} = 123 \mu\text{m}$

- D^{*+} -meson identification:
- topological cuts
 - PID information of the decay particles with ITS, TPC, TOF.

- D-meson daughter tracks are replaced with the D-meson track
- Charged jets reconstruction: FASTJET using the anti- k_T jet finding algorithm with $R = 0.4$, jet p_T corrected for the average background momentum density^[1].
- $p_{T,D^*} > 3$ GeV/c; $|\eta_{jet}| < 0.9 - R$.

D^{*+} -jet reconstruction efficiency

- Reconstruction efficiency of D^{*+} mesons in a jet with $|\eta_{jet}| < 0.5$ vs. D^{*+} -meson p_T from PYTHIA6 + HIJING MC simulation.
- Strong dependence of the efficiency on the D^{*+} -meson p_T due to the topological cuts.
- Weak dependence on the jet p_T .

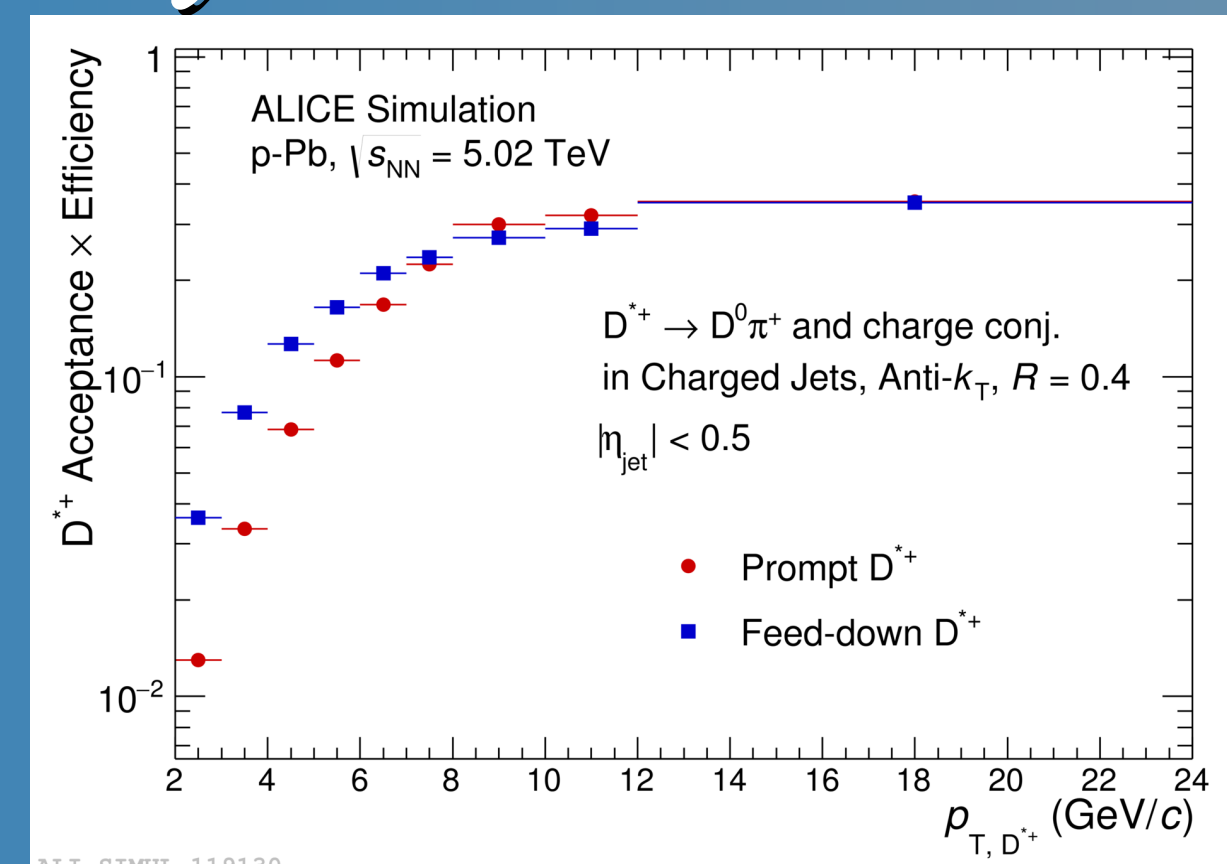


Fig. 1. D^{*+} -jet reconstruction efficiency.

B feed-down subtraction and unfolding

- Raw D^{*+} -jet p_T spectrum is corrected for the B feed-down (FD) contribution according to:

$$\frac{dN_{raw,Prompt}}{dp_{T,jet}} = \frac{dN_{raw}}{dp_{T,jet}} - RM^{FD} \otimes \sum_{p_{T,D^{*+}}} \frac{\epsilon^{FD}(p_{T,D^{*+}})}{\epsilon(p_{T,D^{*+}})} \frac{dN_{sim,FD}}{dp_{T,jet}}(p_{T,D^{*+}})$$

- $\frac{dN_{raw}}{dp_{T,jet}}$: efficiency-corrected raw D^{*+} -jet p_T spectrum
- $\frac{dN_{sim,FD}}{dp_{T,jet}}$: expected yield from POWHEG+PYTHIA simulation for feed-down D^{*+} -jet
- RM^{FD} : feed-down D^{*+} -jet response matrix
- $\frac{\epsilon^{FD}(p_{T,D^{*+}})}{\epsilon(p_{T,D^{*+}})}$: feed-down to prompt D^{*+} -jet efficiency ratio

- And then unfolded: $\frac{dN_{Prompt}}{dp_{T,jet}} = RM^{-1,Prompt} \otimes \frac{dN_{raw,Prompt}}{dp_{T,jet}}$

- RM^{Prompt} : prompt D^{*+} -jet response matrix
- The detector response for prompt D^{*+} -jet from PYTHIA 6 simulations for pp collisions (Fig. 4).
- The background energy-density fluctuations evaluated from the p-Pb data using random cones with $R = 0.4$ (Fig. 5).
- A combined matrix of the detector response and background fluctuations is used at the unfolding step.

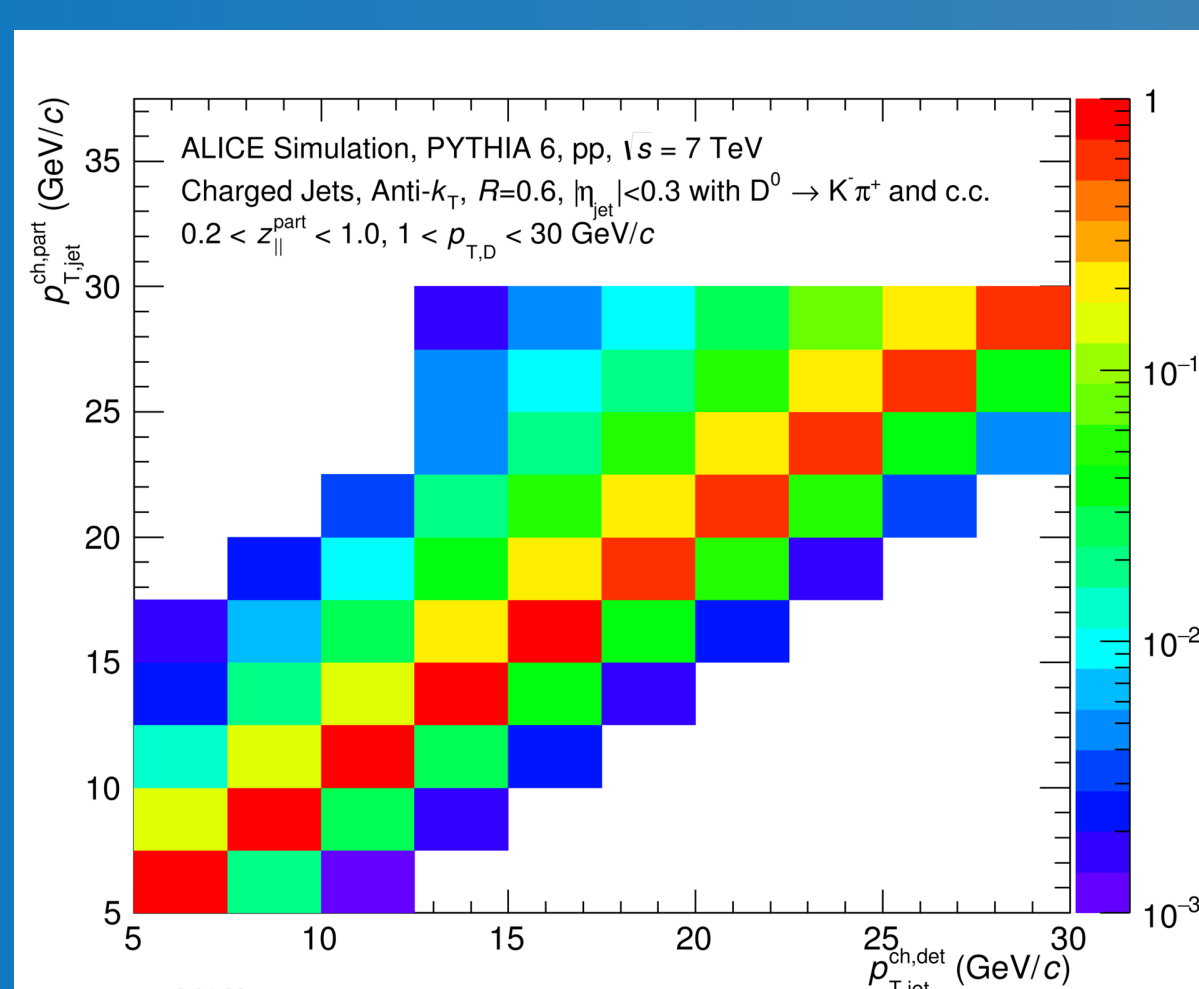


Fig. 4. Detector response matrix for D^0 -jets from MC simulations for pp collisions at $\sqrt{s} = 7$ TeV.

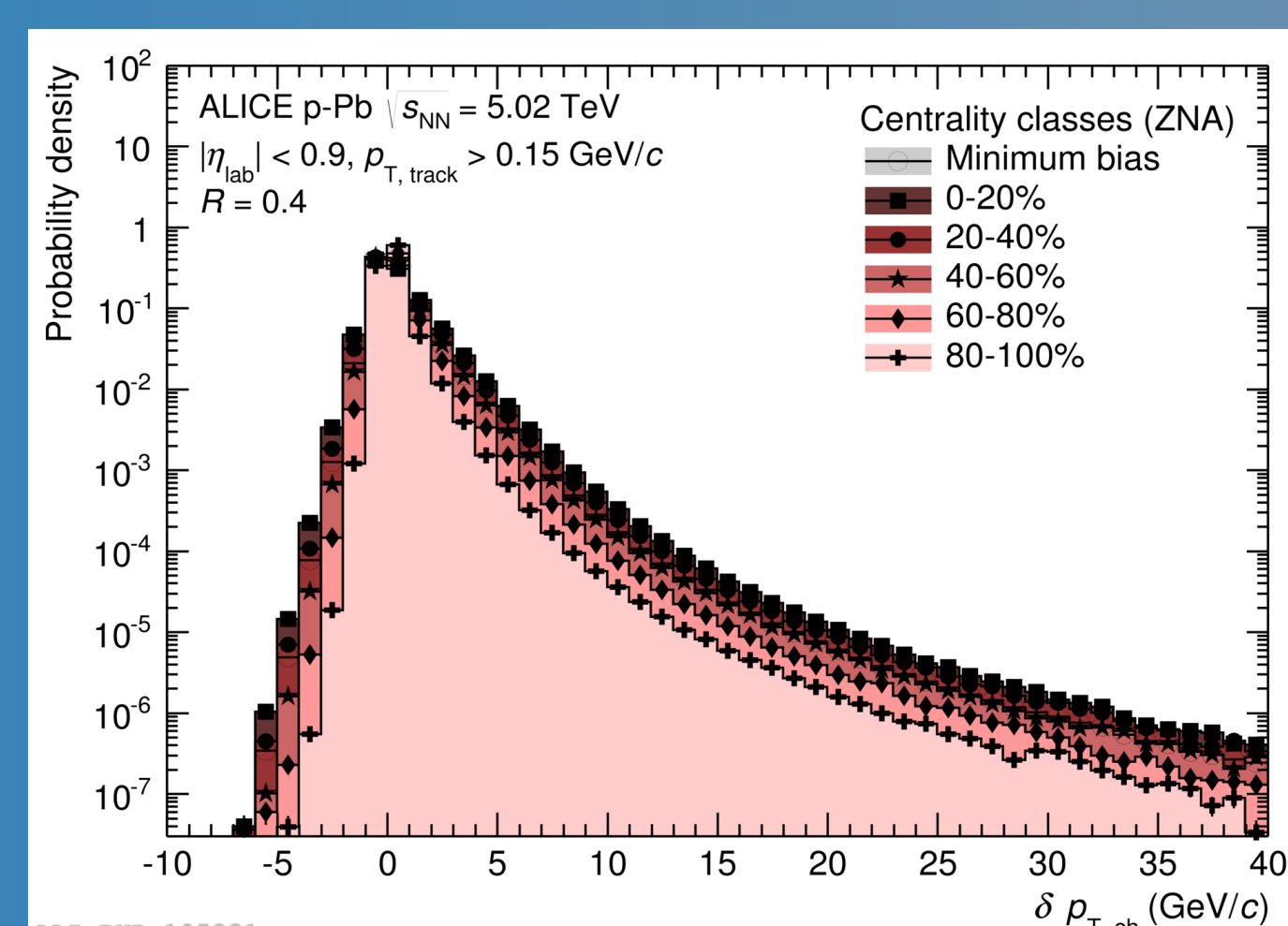


Fig. 5. Background momentum fluctuations of charged jets with random cones ($R=0.4$)^[2].

D^{*+} -tagged jet yields

- D^{*+} -jet yields extracted using D^{*+} -meson invariant mass analysis; 3D distribution: $(p_{T,D^*}, p_{T,jet}, M)$, $M = M(K\pi\pi) - M(K\pi)$

- Two alternative methods:

I) Signal in D^{*+} -meson p_T intervals

- Fit invariant mass distributions in D^{*+} -meson p_T intervals (Fig. 2).
- Define, based on the fit:
 - **Signal region:** $|M - \mu_{fit}| < 3 \sigma_{fit}$
 - **Side Bands:** $-8 \sigma_{fit} < M - \mu_{fit} < -5 \sigma_{fit}$ and $5 \sigma_{fit} < M - \mu_{fit} < 13 \sigma_{fit}$
- **Raw jet p_T distribution:**
 - Subtract the side-band jet p_T distribution $B \frac{dN^{SB}}{dp_{T,jet}}$ from the jet p_T distribution in the signal region $\frac{dN^S}{dp_{T,jet}}$ (B - normalization to the background in the signal region).
 - Correct for the prompt D^{*+} -jet reconstruction efficiency, $\epsilon(p_{T,D^*})$ (Fig. 1) and sum up the D^{*+} -meson p_T intervals.

$$\frac{dN^{raw}}{dp_{T,jet}} = \sum_{p_{T,D^{*+}}} \frac{1}{\epsilon(p_{T,D^{*+}})} \left[\frac{dN^S}{dp_{T,jet}}(p_{T,D^{*+}}) - B \frac{dN^{SB}}{dp_{T,jet}}(p_{T,D^{*+}}) \right]$$

II) Signal in jet p_T intervals

- For every jet p_T interval, correct each D^{*+} -meson candidate by the corresponding prompt D^{*+} -jet efficiency, $\epsilon(p_{T,D^*})$.
- Fit the efficiency-scaled invariant mass distributions in the jet p_T intervals (Fig. 3).
- **Raw jet p_T distribution:**
 - Extract the jet yield from the signal fit in the signal region.

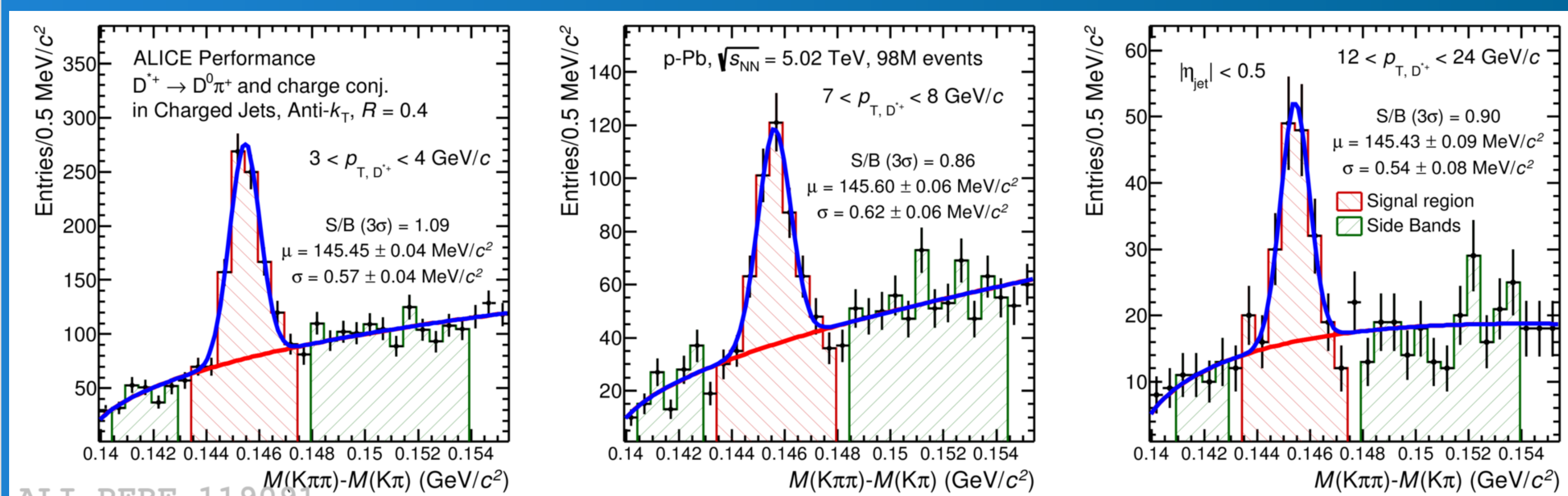


Fig. 2. Invariant mass distributions in D^{*+} -meson p_T intervals, with the signal region and side bands.

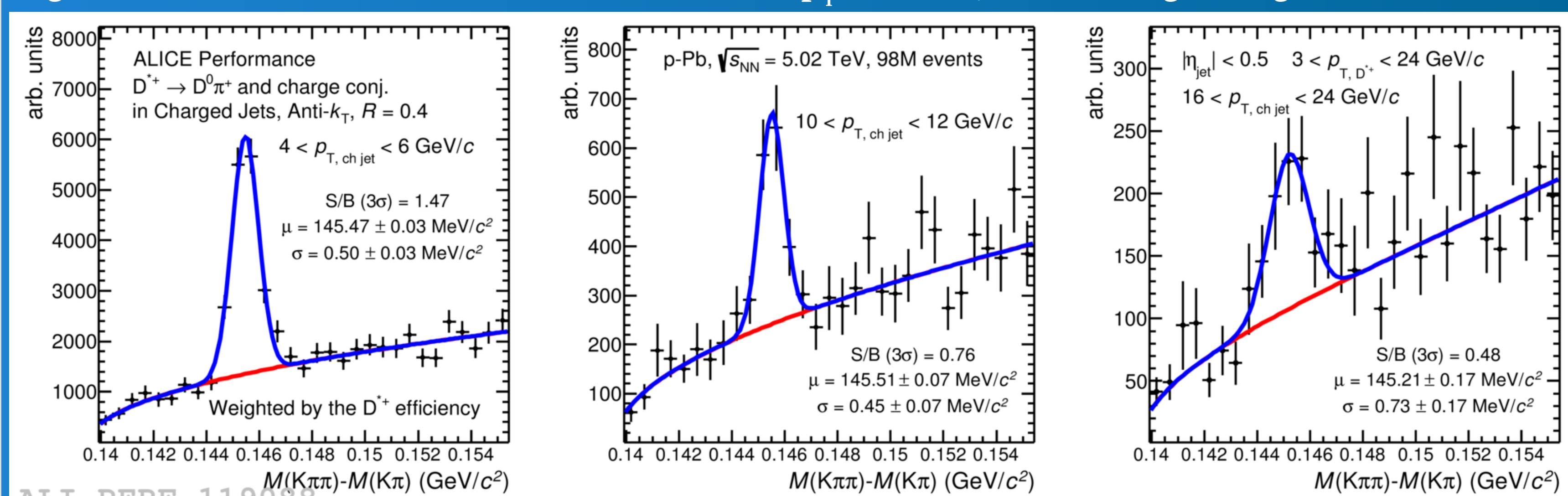


Fig. 3. Invariant mass distributions weighted by the D^{*+} -jet efficiency in jet p_T intervals.

Outlook

- The D^{*+} -tagged charged jets in Run 1 p-Pb collisions at $\sqrt{s_{NN}} = 5.02$ TeV can be measured in the range of $4 < p_T < 24$ GeV/c, with the ALICE detector.
- The final D^{*+} -tagged jet p_T spectrum will provide a reference for D-tagged jet analysis in Pb-Pb collisions.
- The studies will be extended to analysis of the D-meson momentum fraction with respect to the jet, using also the Run 2 p-Pb dataset at $\sqrt{s_{NN}} = 5.02$ TeV.

[1] S. Chatrchyan et al. (CMS Collaboration), JHEP 1208 (2012) 130
[2] J. Adam et al. (ALICE Collaboration), Eur. Phys. J. C76 (2016) no.5, 271